

## Electronic Supplementary Information

### Synthesis and characterization of zirconia-grafted SBA-15 nanocomposites

Benjamin Katryniok, Sébastien Paul, Mickael Capron, Sébastien Royer, Christine Lancelot, Louise Jalowiecki-Duhamel, Virginie Bellière-Baca, Patrick Rey, and Franck Dumeignil

### Index

<b>Figure S1:</b> Low angle XRD for SBA-15 silica host supports with pore size of 9 nm (a); 8 nm (b), 6 nm (c); 5 nm (d) and 4 nm (e).....	2
<b>Figure S2:</b> Distribution of the pore diameter of the SBA-15 supports with a pore size of 4 nm (□), 5 nm (◇), 6 nm (Δ), 8 nm (x) and 9 nm (+).....	2
<b>Figure S3:</b> Nitrogen adsorption-desorption isotherm hysteresis loops for the initial SBA-15 (□), 20Zr-SBA8nm-c400 (◇), 20Zr-SBA8nm-c650 (Δ), 20Zr-SBA8nm-c950 (x) samples. ....	3
<b>Figure S4:</b> Low angle XRD patterns for different calcination temperatures; 0Zr-SBA8nm-c25 (a), 20Zr-SBA8nm-c400 (b), 20Zr-SBA8nm-c650 (c), 20Zr-SBA8nm-c950 (d) and 0Zr-SBA8nm-c950 (e). .....	3
<b>Figure S5:</b> Nitrogen adsorption isotherms and BJH pore distribution for initial 0Zr-SBA8nm-c25 (Δ), 10Zr-SBA8nm-c650 (□), 20Zr-SBA8nm-c650 (◇) and 40Zr-SBA8nm-c650 (x) samples.....	3
<b>Figure S6:</b> Low angle XRD patterns for different zirconia amounts; 0Zr-SBA8nm-c25 (a), 10Zr-SBA8nm-c650 (b), 20Zr-SBA8nm-c650 (c) and 40Zr-SBA8nm-c650 (d). .....	4
<b>Figure S7:</b> Low angle XRD of 20Zr-SBA9nm-c650 (a); 20Zr-SBA8nm-c650 (b), 20Zr-SBA6nm-c650 (c); 20Zr-SBA5nm-c650 (d) and 20Zr-SBA4nm-c650 (e) .....	4

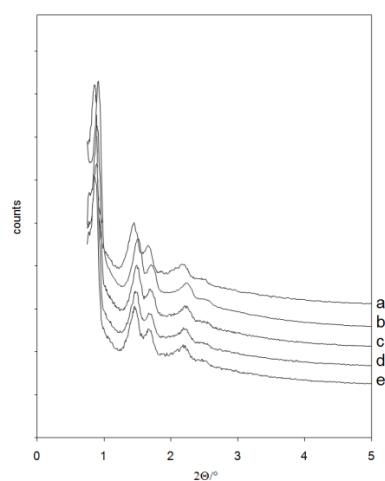


**Figure S1:** Low angle XRD for SBA-15 silica host supports with pore size of 9 nm (a); 8 nm (b), 6 nm (c); 5 nm (d) and 4 nm (e).

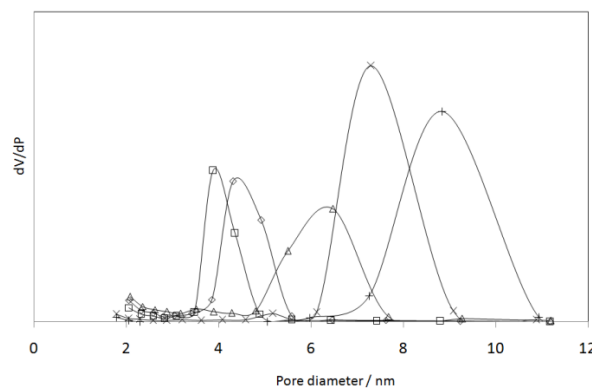


**Figure S2:** Distribution of the pore diameter of the SBA-15 supports with a pore size of 4 nm ( $\square$ ), 5 nm ( $\diamond$ ), 6 nm ( $\Delta$ ), 8 nm (x) and 9 nm (+).

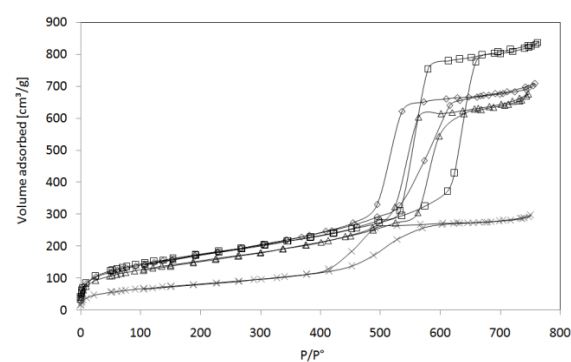


**Figure S3:** Nitrogen adsorption-desorption isotherm hysteresis loops for the initial SBA-15 ( $\square$ ), 20Zr-SBA8nm-c400 ( $\diamond$ ), 20Zr-SBA8nm-c650 ( $\Delta$ ), 20Zr-SBA8nm-c950 (x) samples.

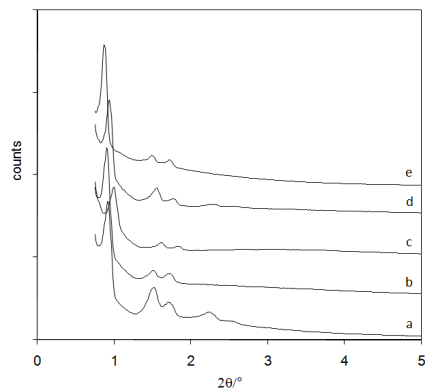


**Figure S4:** Low angle XRD patterns for different calcination temperatures; 0Zr-SBA8nm-c25 (a), 20Zr-SBA8nm-c400 (b), 20Zr-SBA8nm-c650 (c), 20Zr-SBA8nm-c950 (d) and 0Zr-SBA8nm-c950 (e).

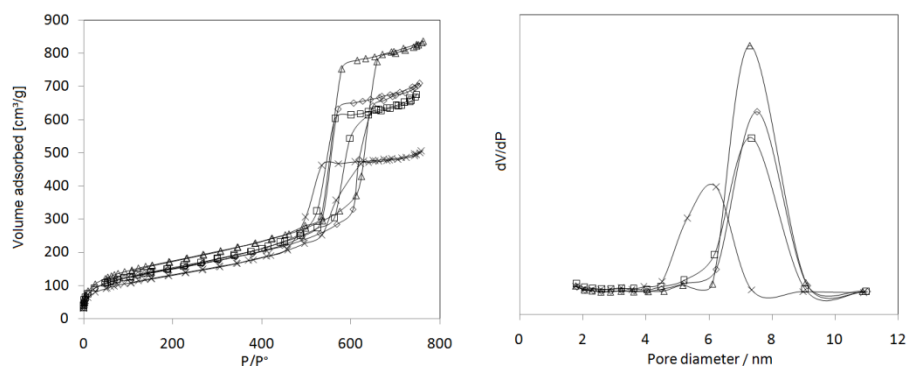


**Figure S5:** Nitrogen adsorption isotherms and BJH pore distribution for initial 0Zr-SBA8nm-c25 ( $\Delta$ ), 10Zr-SBA8nm-c650 ( $\square$ ), 20Zr-SBA8nm-c650 ( $\diamond$ ) and 40Zr-SBA8nm-c650 (x) samples.

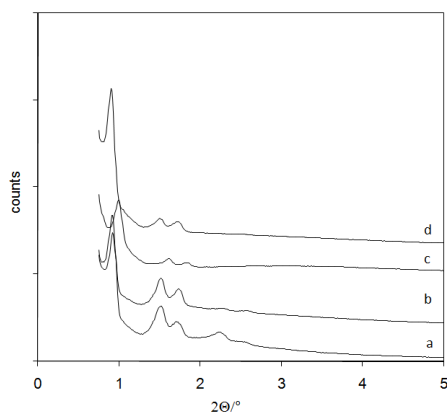


**Figure S6:** Low angle XRD patterns for different zirconia amounts; 0Zr-SBA8nm-c25 (a), 10Zr-SBA8nm-c650 (b), 20Zr-SBA8nm-c650 (c) and 40Zr-SBA8nm-c650 (d).

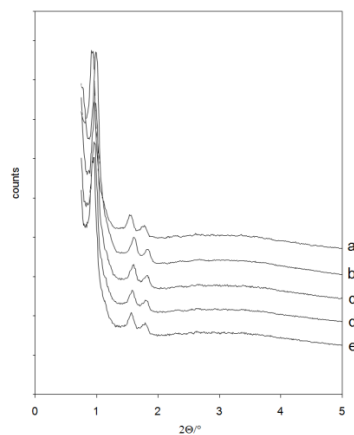


**Figure S7:** Low angle XRD of 20Zr-SBA9nm-c650 (a); 20Zr-SBA8nm-c650 (b), 20Zr-SBA6nm-c650 (c); 20Zr-SBA5nm-c650 (d) and 20Zr-SBA4nm-c650 (e).